Electronic Supporting Information

Rapid Gram-Scale Synthesis of Au/Chitosan Nanoparticles Catalysts by Using Solid-Mortar Grinding

K. Paul Reddy[1], R. S. Meerakrishna[2], P. Shanmugam[2], Biswarup Satpati[3] and A. Murugadoss[1]*

[1]Department of Inorganic Chemistry, University of Madras, Guindy Campus, Chennai – 600025, India. E–mail: murugadoss@unom.ac.in; ammuruga@gmail.com

[2]Organic and Bioorganic Chemistry Division, Council of Scientific and Industrial Research (CSIR) – Central Leather Research Institute (CLRI), Adyar, Chennai – 600020, India.

[3]Surface Physics and Material Science Division, Saha Institute of Nuclear Physics, Kolkata – 700064, India.

1. Experimental details

1.1. General

UV–visible spectra of samples were recorded using a Varian Cary 100 Bio Dual beam spectrophotometer in the range of 200–800 nm. The High–resolution Transmission electron microscopy (HR–TEM) images of supported gold Nanoparticles (NPs) were carried out using FEL, TF30–ST equipment operating at an acceleration voltage of 300 kV. The concentration of Au content was measured by the ICP–OES (Prodigy XP ICP–OES). X–ray photoelectron spectroscopy of chit-Au1 was measured by VG Scientific ESCALAB 250. FTIR spectra of metal nanoclusters obtained from the FTIR 4700 typeA model. ^{1}H and ^{13}C NMR spectra were recorded using a Bruker spectrometer at 400 MHz, $CDCl_3$ or DMSO–d_6 was used a

solvent and the residual solvent peak was used an internal standard (7.26 ppm for $CDCl_3$ and 2.50 ppm for DMSO–d_6). TLC analysis was performed using Merck Silica gel 60 F_{254}.

1.2. Materials

All chemicals and solvents were used as received without further purifications. Hydrogen tetrachloroaurate ($HAuCl_4$ 99.99%, from Alfa–Aesar), Chitosan (poly (D–glucosamine)) with a medium molecular weight of 75–85 % deacetylated was from sigma Aldrich, Poly(vinyl alcohol) (PVA, n = approx. 1700, from TCI), Sodium borohydride ($NaBH_4$, 95%, from Merck), *p*–Nitrothiophenol (from TCI), Glycol Acetic acid (CH_3COOH, 99–100%, from Merck), Potassium carbonate (K_2CO_3, from SDFCL), and Anhydrous Sodium sulphate (Na_2SO_4, from Fisher scientific). All the substrates (phenylboronic acid its derivates and benzyl alcohol and its derivates are received from TCI), Ethyl acetate and Hexane were purchased from Finar Chemicals. DD water was used in all experiments. All Glassware's were cleaned with non–ionic detergent followed by DD water and raised with DD water prior to usage.

1.3. General procedure for preparation of solid chitosan supported gold NPs by Solid-Grinding

A given amount of solid chitosan was mixed with $HAuCl_4$ were grounded in a mortar at room temperature for two minutes. To this yellow colour solid mixtures, the solid $NaBH_4$ (19 mg, 0.5 mmol) was added and the grinding was continued for another five minutes. The solid mixture colour changes from yellow to dark gray indicating the formation of gold NPs. The resulting powder was washed with double distilled water by simple (Whatman 40) filter paper in several times until the filtered pH reach to neutral. The amount of solid chitosan and $HAuCl_4$ used for the preparation of chit-Au1, chit-Au2, chit-Au3 and chit-Au4 samples were

given in the table 1 (main text). The amount of solid $NaBH_4$ was maintained as 0.5 mmol in all sample preparations.

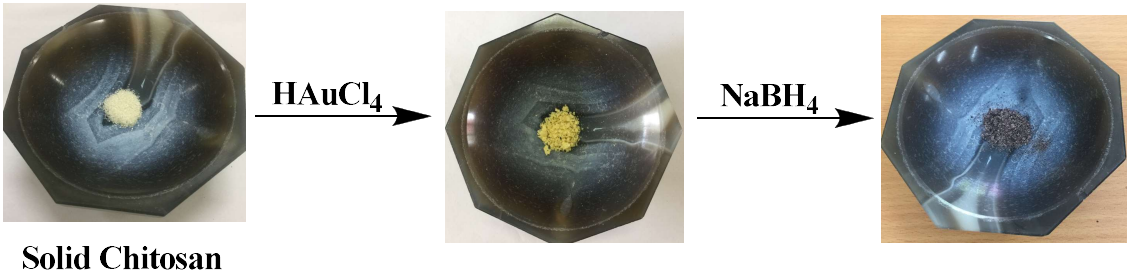

Scheme 1. *Photography indication of colour changes during the preparation of chitosan supported gold NPs.*

Figure S1. *Purification and washing of chitosan supported gold NPs by using simple filter paper.*

1.4. Synthesis of chitosan stabilized gold NPs by solution based method

Solid chitosan (0.837 mmol) was dissolved in aqueous acetic acid solution 1 % (v/v). To this 85 µL of $HAuCl_4$ (0.02 mmol) was added and the resulting mixture was stirred for 30 min at 1600 rpm in room temperature. Then aqueous $NaBH_4$ (19 mg, 2.5 mL, 0.5 mmol) was

added rapidly to this mixtures and stirring was continued for another 20 min. The resultant reaction mixture slowly turned into dark red gel, indicating the formation of gold NPs in the gel[1].

This observation indicates that due to inherent viscous nature of chitosan polymer, it is very difficult to scale up for the synthesis of chitosan stabilized gold NPs in solution based methods.

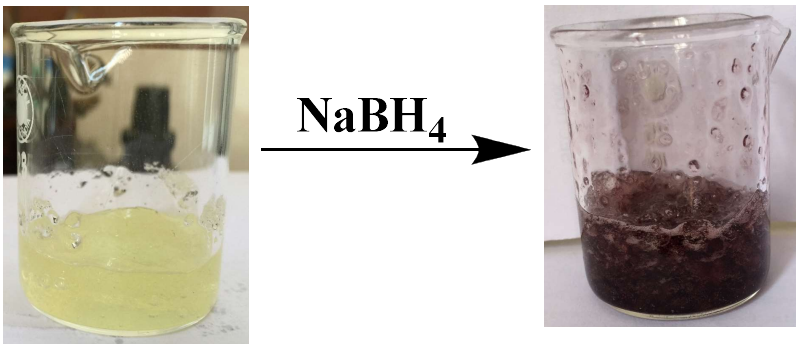

Figure S2*. Chitosan stabilized gold NPs gel formation by solution based methods.*

1.5. Determination of gold content in solid chitosan supported gold NPs

Solid chitosan supported gold NPs was dissolved in the aqua regia solutions (1:1 aqua regia and water) were allowed to react at room temperature for overnight, which results complete dissolution of gold NPs into gold ions. The resulting samples were analysed by ICP-OES. Content of gold in the chitosan support determined in each samples were shown in table 1 (main text).

1.6. Reproducibility

The synthesis of solid chitosan supported gold NPs catalysts by physical mixing of gold chloride and $NaBH_4$ with the chitosan support in pestle and mortar was reproducible for several times as shown in Figure S3.

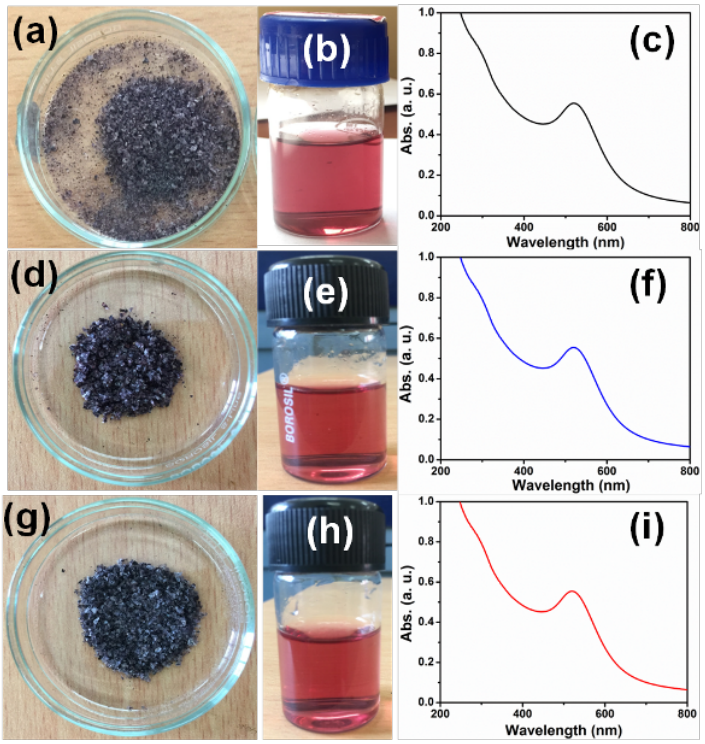

Figure S3. *The reproducibility of preparation of solid chitosan supported gold NPs by solid-grinding (a)-(c) 1st time, (d)-(f) 5th time and (g)-(i) 10th time.*

2. Characterization of solid chitosan supported gold NPs

2.1. UV-Visible spectroscopy: The obtained solid chitosan supported gold NPs from solid-grinding were dissolved in 1% aqueous acetic acid solution. The absorption spectra of the resulting solutions were analyzed under ambient conditions.

2.2. Transmission Electron Microscopy: A pinch of solid chitosan supported gold NPs were dispersed in Milli-Q water was drop coated on the carbon coated copper grid (400 Mesh) and allowed for air-drying. A coated grid was then analysed by TEM under the magnification of 100,000-120,0000X.

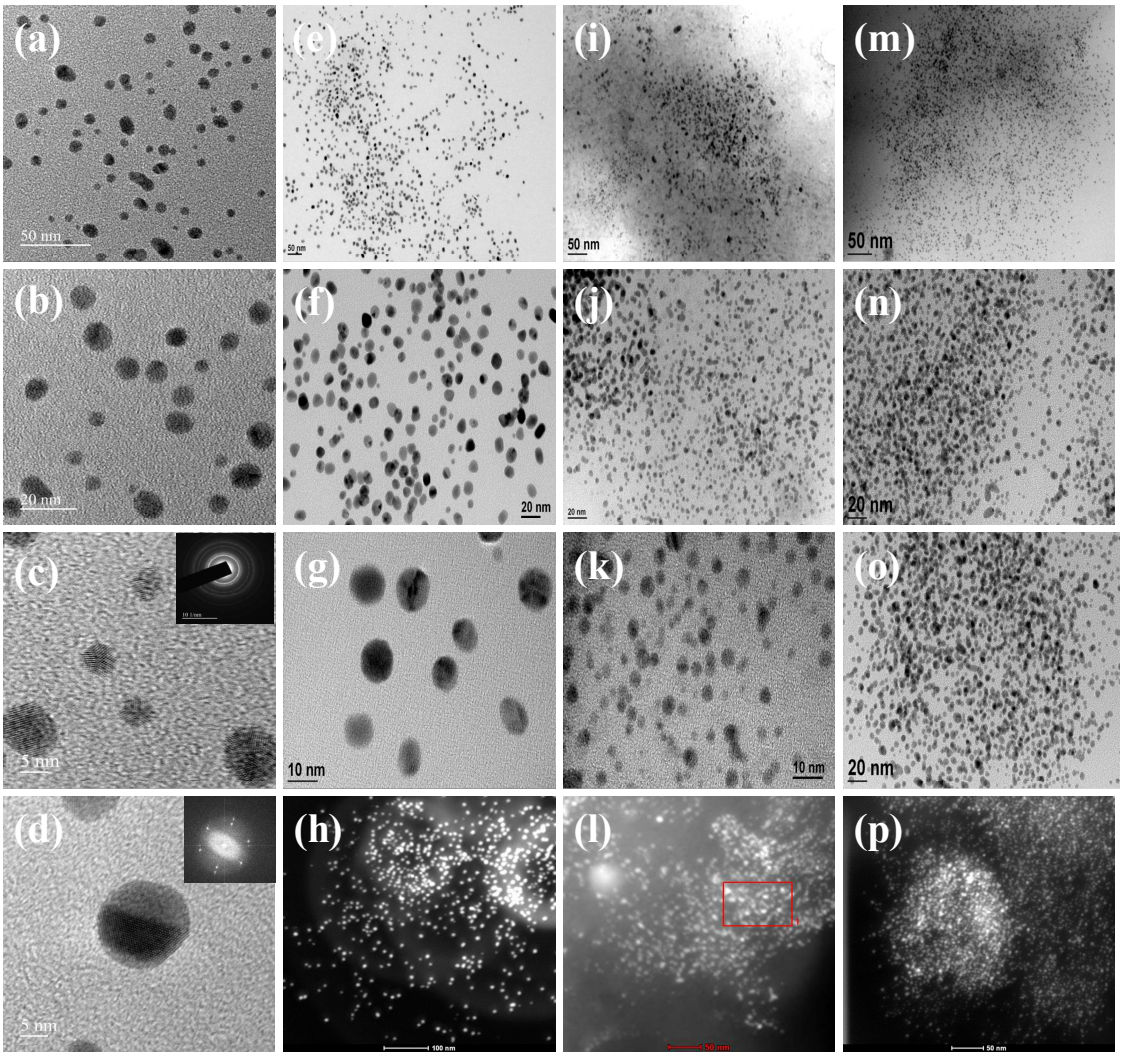

Figure S4*. TEM and HRTEM images of (a) to (c) Chit–Au 1 catalysts (insert figure in the C is corresponding SAED pattern of gold NPs and (d) Lattice fringes and corresponding FFT (inset) pattern of gold NPs. (e) to (h) TEM and HAADF images of Chit–Au 2, (i) to (l) Chit–Au 3, and (m) to (p) Chit–Au 4 samples.*

2.3. Fourier-transform infrared spectroscopy: 2 mg of chitosan or solid chitosan supported gold NPs were mixed with 8 mg of solid KBr. After grounding this mixtures using pestle and mortar at temperature, the pallatte was made, which was then analyzed under FTIR in transmission mode in ambient condition.

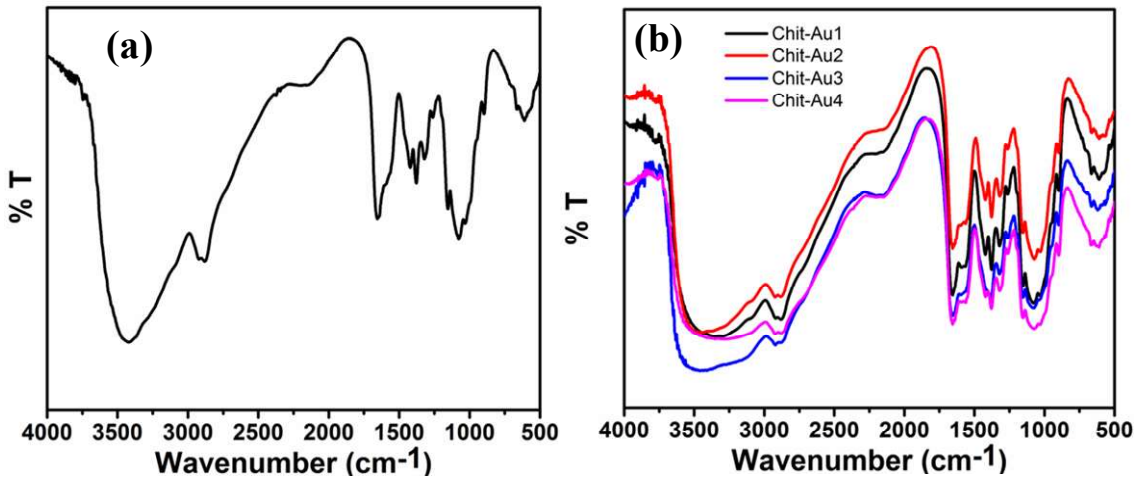

Figure S5. *FTIR spectra (a) only* chitosan *and (b) chitosan supported gold NPs.*

2.4. X-ray photoelectron spectra of Chit-Au1: solid chit-Au1 powder was dispersed on the graphitic carbon tape was analyzed by XPS. The base pressure in the analyzer was ca. 2×10^{-9} Torr. X-rays from the Mg Kα line at 1253.6 eV (15 kV, 20 mA) were used for excitation. Photoelectrons were corrected in the constant analyzer energy mode with pass energy of 50 eV. The overall resolution was 1 eV for the XPS measurements. The core level binding energies (BE) were calibrated using graphitic carbon tap with the adventitious carbon binding energy of 286.2 eV.

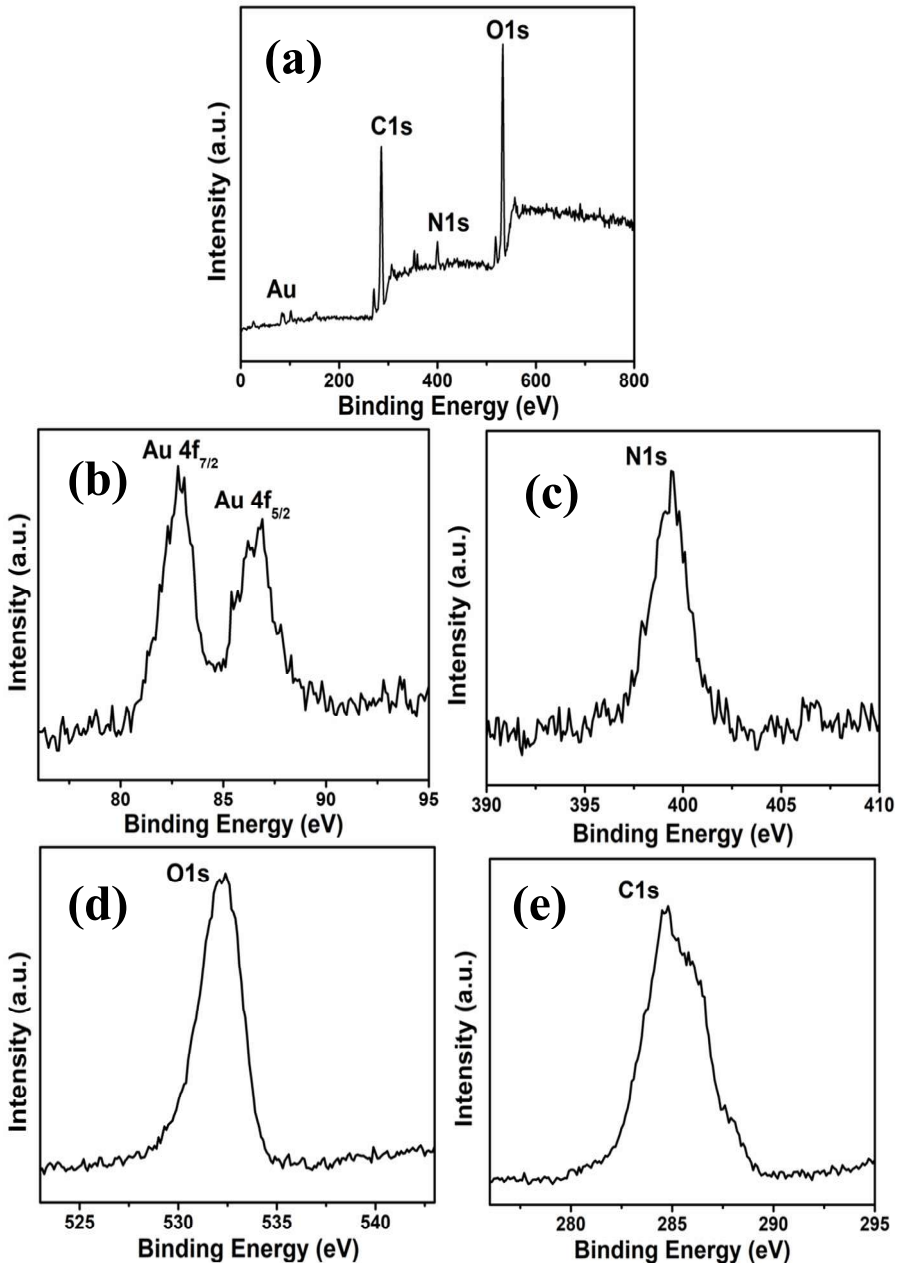

Figure S6. *Representative XPS spectra of chit-Au1 (a) full range and core level spectra of (b) Au 4f, (c) N1s, (d) O1s and C1s (e).*

2.5. XANES and EXAFS study of chit-Au1: Au L_3–edge x–rays absorption near edge structure (XANES) spectra were recorded at BL–9, scanning extended edge x–rays absorption fine structure (EXAFS) Beamline of Indus–2 [http://iopscience.iop.org/article/10.1088/1742-6596/493/1/012032/meta]. XAFS measurements of film were done in transmission mode. The beamline consists of Rh/Pt coated meridional cylindrical mirror for collimation and Si (111) based double crystal monochromator to select excitation energy. The energy range of XAFS was calibrated using Au metal foil at 11919 eV. The analysis of the XAFS data have been carried out following the standard procedures using the IFEFFIT software package, which includes Fourier transform (FT) to derive the χ(R) versus R plots from the absorption spectra using ATHENA software, generation of the theoretical EXAFS spectra starting from an assumed crystallographic structure using ARTEMIS software[2] and finally fitting of χ(R) versus R experimental data with the theoretical ones using the FEFF 6.0 code[3].

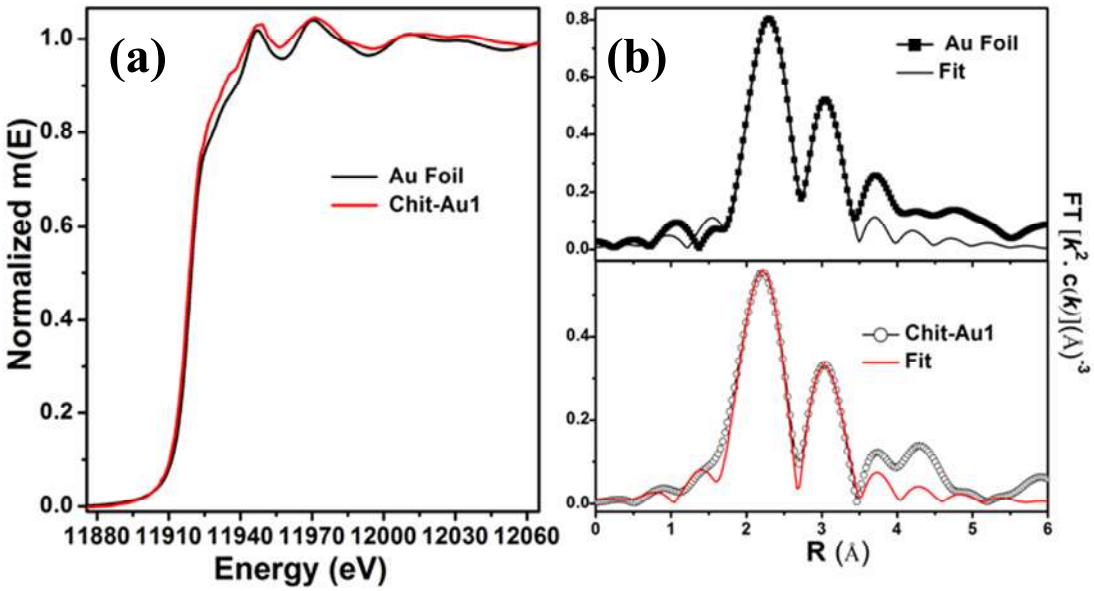

Figure S7*. (a) XANES spectra of Chit–Au1 at Au L_3–edge and Au L_3 EXAFS in κ space (b).*

2.6. Calculation of the available surface area of the Chit –Au NPs: To prepare the standard calibration curve of the *p*–nitrothiophenol (*p*–NTP), a known concentration of aqueous solution of *p*–NTP was prepared by diluting the 1 mM stock solution at room temperature[4-5]. Then, fixed amount of sold chitosan supported gold NPs (2 mg) was mixed with various amount of 1 mM stock solution of *p*–NTP solutions. The mechanical stirrer at 500 rpm was used to shake this mixture. The mixtures were then filtrated and the resulting solution was collected in a separate vial to measure the unadsorbed amount of *p*–NTP using the extinction coefficient of *p*–NTP. The equilibrium concentration was calculated from the absorbance peak intensity after adsorption. The moles of adsorbed *p*–NTP per gram of Chit–Au NPs were calculated by dividing the total amount of adsorbed *p*–NTP by weight of gold present in the supported gold NPs solution. The adsorption isotherm was then generated by dividing the number of moles of adsorbed *p*–NTP per gram of gold present in the chitosan support (As mentioned above, the content of gold present in the chitosan support was determined from ICP-OES analysis) with the equilibrium concentration of *p*–NTP. The Langmuir isotherm is a relationship between the equilibrium concentrations of *p*–NTP divided by adsorbed moles of *p*–NTP per gram of Chit–Au NPs versus the equilibrium of concentration of *p*–NTP (Fig. 3b main text). The slope of the Langmuir plot will give the reciprocal of the number of moles of *p*–NTP per gram of gold on the chitosan support, so the active surface area can be calculated using the following equation:

$$\text{Surface area} = 1/\text{slope} \times (N_A) \times 0.187 \times 10^{-18}\ m^2$$

Where N_A is Avogadro's number and the value of $0.187 \times 10^{-18}\ m^2$ is area of *p*–NTP.

3. Catalytic study

3.1. General Procedure for homo coupling reaction of phenylboronic acid and its derivatives catalyzed by solid chitosan supported gold NPs:

To a 25 mL round bottom flask containing a mixture of phenylboronic acid and its derivatives (0.25 mmol), solid chitosan supported gold catalysts (0.15 g catalysts) and DD water (15 mL) were stirred (1200 rpm) under air at room temperatures. The reaction progress was monitored by thin layered chromatographic (TLC) analysis. The catalysts were separated by filtration and washed with ethyl acetate (8 mL x 3). The reaction mixture was quenched with 10 mL of 3 N HCL and then extracted with ethyl acetate (3×15 mL). The organic layer was dried over anhydrous Na_2SO_4 and evaporated in vacuum. The crude product was purified by column chromatography (5% Ethyl acetate in hexane) to provide pure product. The isolated yield was then determined after complete drying in high vacuum. The product was confirmed by ^{1}H and ^{13}C NMR spectra.

3.2. Homocoupling reaction of phenylboronic acid catalyzed by chitosan stabilized gold NPs gel:

Chitosan stabilized gold NPs gel prepared by solution based methods was tested as heterogeneous catalysts for the homocoupling of phenylboronic acid under air in water at room temperature. As shown in table S1, this catalyst showed inferior catalytic activity. Therefore, it can be concluded that due inherent viscous nature of chitosan polymer not only hinder the preparation of chitosan stabilized gold NPs in gram scale but also strongly affect the catalytic activity.

Table S1. *Homocoupling reaction of phenylboronic acid catalyzed by chitosan stabilized gold NPs gel.*

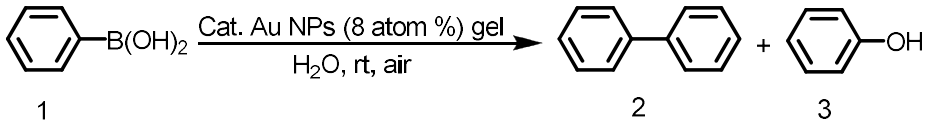

Entry	Time (h)	Yield (%)[b]	
		2	3
1	48	ND	ND

[a]Reaction conditions: substrate (0.25 mmol), water (15 mL), chitosan 0.84 mmol, and Au (0.02 mmol). [b]Isolated yields

3.3. General Procedure for benzyl alcohols and its derivatives catalyzed by solid chitosan supported gold NPs:

To a 25 mL round bottom flask containing a mixture of benzyl alcohol and its derivatives (0.25 mmol), K_2CO_3 (103.6 mg, 0.75 mmol), solid chitosan supported gold catalysts (0.15 g catalysts) and DD water (15 mL) were stirred (1200 rpm) under air at room temperature. The reaction progress was monitored by thin layered chromatographic (TLC) analysis. The catalysts were separated by filtration and washed with ethyl acetate (8 mL x 3). The reaction mixture was quenched with 10 mL of 3 N HCL and then extracted with ethyl acetate (3×15 mL). The organic layer was dried over anhydrous Na_2SO_4 and evaporated in vacuum. The crude product was purified by column chromatography (5% Ethyl acetate in hexane) to provide pure product. The isolated yield was then determined after complete drying in high vacuum. The product was confirmed by ^1H and ^{13}C NMR spectra.

3.4. Reusability test of solid chitosan supported gold NPs

Reusability of solid chitosan supported gold NPs catalysts (0.15 gram catalysts (0.02 mmol gold (Au) and 0.834 mmol chitosan)) were tested for both homocoupling of *4*–methylphenylboronic acid, *p*–hydroxybenzyl alcohol under the reaction condition as mentioned in the entry 2 and 8 of table 2 and 3 in the main text. After completion of each cycle the catalyst recovered by centrifuged, washed with water several times and dried at room temperature then used for the consequent cycles.

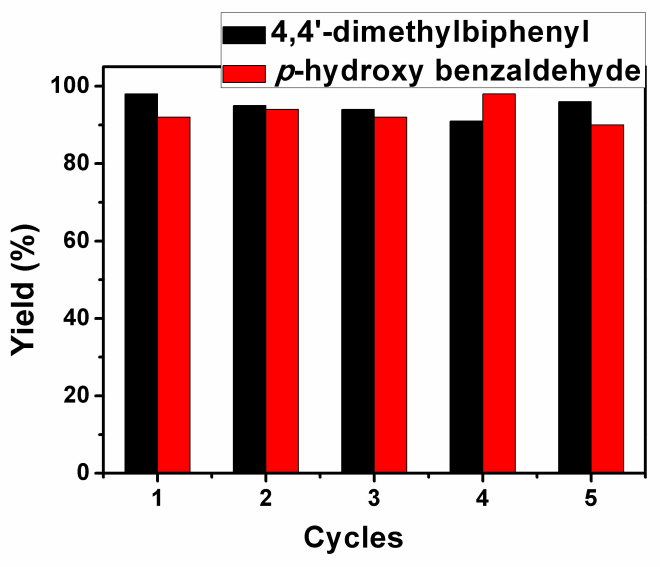

Figure S8. *Product yields of 4,4'–dimethylbiphenyl and p–hydroxyl benzaldehyde after each cycle of catalytic reaction.*

3.5. Characterization of the recovered chitosan supported gold catalysts after fifth cycles:

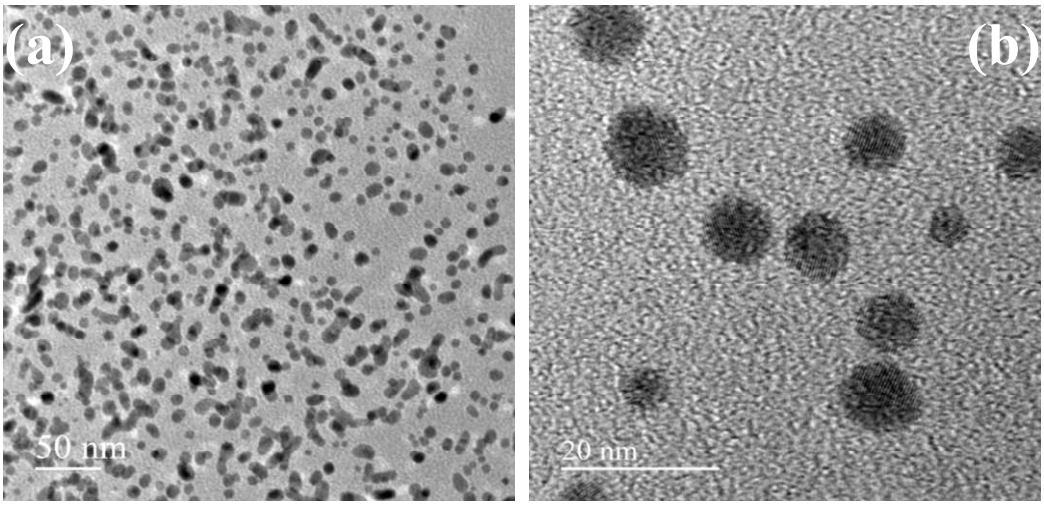

Figure S9. *TEM images of reused solid chitosan supported gold NPs catalysts after fifth cycles*

3.6. Preparation of Au/PVA and Au/PVP catalysts by Solid grinding:

The mixture of solid PVP (0.093 g, MW 40K) and PVA (0.072 g Medium MW) and $HAuCl_4$ (0.02 mmol) were grounded in a mortar at room temperature for two minutes. To this yellow colour semi-solid mixtures. The solid $NaBH_4$ (19 mg, 2.5 mL, 0.5 mmol) was added and the grinding was continued for another five minutes. The solid mixture colour changes from yellow to dark greyish black indicating the formation of gold NPs. The resulting powder was washed with double distilled water by simple (Whatman 40) filter paper in several times until the filtered pH reach to neutral.

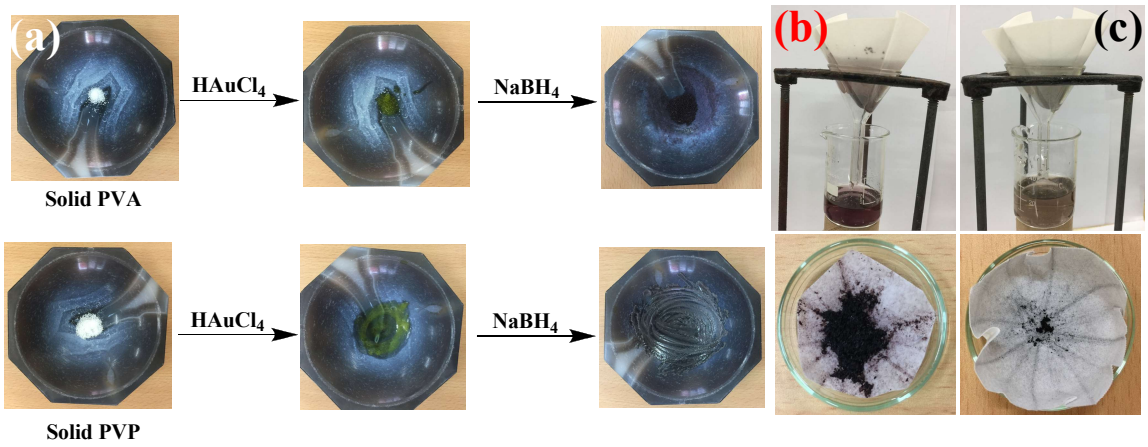

Figure S10. *(a) Photography indication of colour changes during the preparation of PVA and PVP supported Au NPs. (b) and (c) are purification and washing of PVA and PVP supported Au NPs, respectively by using simple filter paper.*

As shown in the Figure S10 (b) and (c), the Au NPs are leached out from the polymer support during washing and purification process indicating that these polymers are incapable to stabilize the Au NPs effectively during the solid grinding. Both filtrates and washed precipitates of PVA and PVP supported Au NPs were tested for homocoupling of phenylboronic acid under the same reaction conditions as mentioned in entry 1 (table 2, main text). It was observed that both filtrates and washed precipitates of PVA and PVP supported Au NPs exhibits inferior catalytic activity toward homocoupling of phenylboronic acids (Table S2).

Table S2. Homocoupling of phenylboronic acids catalyzed by solid polymer supported gold NPs[a].

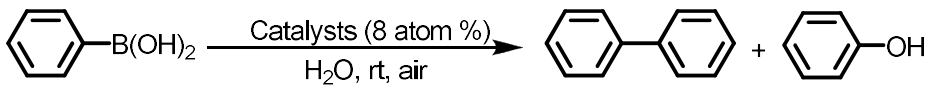

1 2 3

Entry	Catalyst	Time (h)	Yield (%)[b]	
			2	**3**
1	Au/PVA (solid powder)	1 3 5	ND	ND
2	Au/PVA (Mother liquid)	1 3 5	ND	ND
3	Au/ PVP (solid powder)	1 3 5	ND	ND
4	Au/PVP (Mother liquid)	1 3 5	ND	ND

4. NMR spectral data of products

Biphenyl: ^{1}H NMR (400 MHz, $CDCl_3$) δ 7.63 – 7.56 (m, 4H), 7.48 – 7.40 (m, 4H), 7.38 – 7.31 (m, 2H); ^{13}C NMR (100 MHz, $CDCl_3$): δ 141.2, 128.7, 127.2.

4, 4'- Dimethylbiphenyl: ^{1}H NMR (400 MHz, $CDCl_3$) δ 7.50 – 7.45 (m, 4H), 7.26 – 7.21 (m, 4H), 2.39 (s, 6H); ^{13}C NMR (100 MHz, $CDCl_3$): δ 138.2, 136.7, 129.4, 126.8, 21.1.

4, 4'- Dimethoxybiphenyl: ^{1}H NMR (400 MHz, $CDCl_3$) δ 7.50 – 7.45 (m, 4H), 6.98 – 6.93 (m, 4H), 3.84 (s, 6H); ^{13}C NMR (100 MHz, $CDCl_3$): δ 158.6, 133.5, 127.7, 114.8, 55.3.

4, 4'- Difluorobiphenyl: ^{1}H NMR (400 MHz, $CDCl_3$) δ 7.53 – 7.46 (m, 4H), 7.16 – 7.08 (m, 4H); ^{13}C NMR (100 MHz, $CDCl_3$): δ 163.6, 161.2, 136.4, 128.5, 115.6.

4, 4'- Dicholorobiphenyl: ^{1}H NMR (400 MHz, $CDCl_3$) δ 7.50 – 7.46 (m, 4H), 7.42 – 7.39 (m, 4H), 7.20 – 7.17 (m, 1H), 6.79 – 6.75 (m, 1H); ^{13}C NMR (100 MHz, $CDCl_3$): δ 154.3, 138.4, 133.7, 129.5, 129.0, 128.2, 116.6.

4, 4'- Dicyanobiphenyl: ^{1}H NMR (400 MHz, $CDCl_3$) δ 7.74 – 7.70 (m, 4H), 7.65 – 7.61 (m, 4H); ^{13}C NMR (100 MHz, $CDCl_3$): δ 143.5, 132.9, 127.9, 118.4, 112.4.

Benzoic acid: ^{1}H NMR (400 MHz, $CDCl_3$) δ 8.08 – 8.03 (m, 2H), 7.58 – 7.52 (m, 1H), 7.41 (t, J = 7.7 Hz, 2H); 13C NMR (100 MHz, $CDCl_3$): δ 171.9, 133.7, 130.2, 129.3, 128.4.

4-Hydroxybenzaldehyde: ^{1}H NMR (400 MHz, DMSO) δ 10.00 (s, 1H), 9.72 (s, 1H), 7.65 (d, J = 7.9 Hz, 2H), 6.87 (d, J = 8.0 Hz, 2H); ^{13}C NMR (100 MHz, DMSO): δ 190.7, 163.5, 132.1, 128.6, 116.0.

4-Nitrobenzoic acid: ^{1}H NMR (400 MHz, DMSO) δ 8.32 (d, J = 8.1 Hz, 2H), 8.16 (d, J = 8.1 Hz, 2H); ^{13}C NMR (100 MHz, DMSO): δ 166.3, 150.4, 136.9, 131.1, 124.1.

1- Indanone: ^{1}H NMR (400 MHz, $CDCl_3$) δ 7.69 (dd, J = 7.7, 0.4 Hz, 1H), 7.51 (td, J = 7.5, 1.2 Hz, 1H), 7.42 – 7.39 (m, 1H), 7.31 – 7.27 (m, 1H), 3.09 – 3.05 (m, 2H), 2.63 – 2.60 (m, 2H); ^{13}C NMR (100 MHz, $CDCl_3$): δ 207.0, 155.1, 137.1, 134.5, 127.2, 126.6, 123.7, 36.2, 25.8.

5. Scan copies of NMR spectra

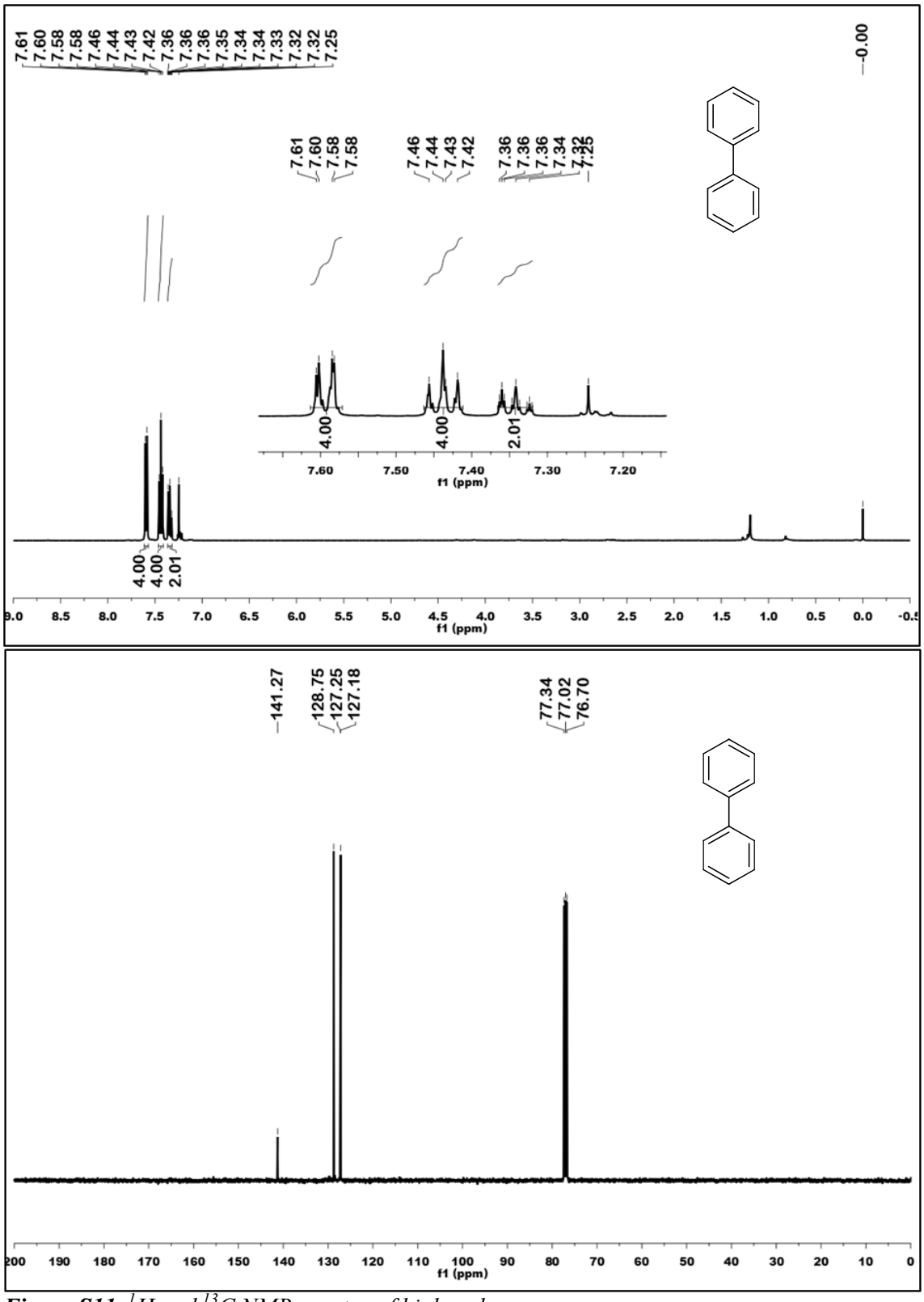

Figure S11. *^{1}H and ^{13}C NMR spectra of biphenyl*

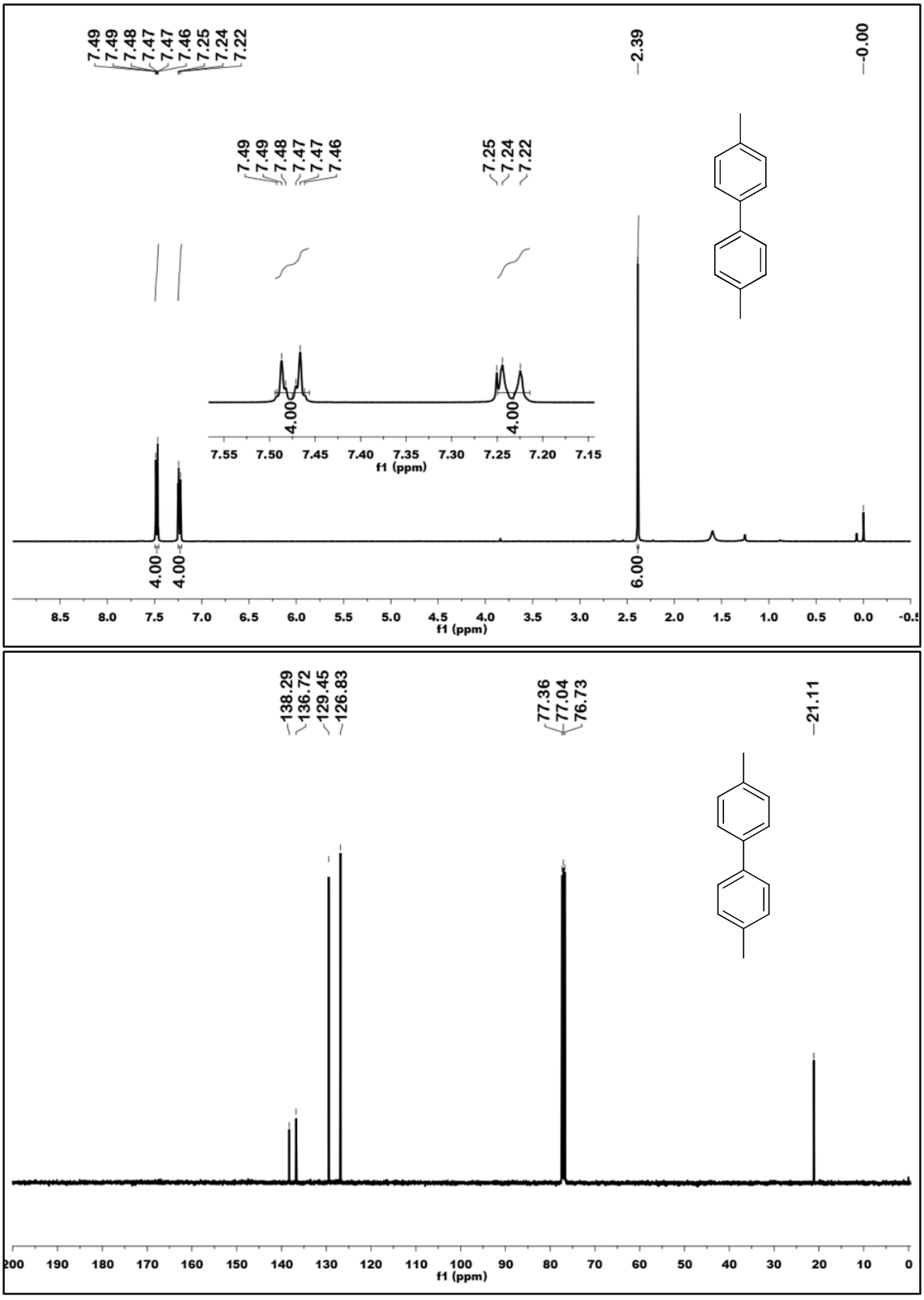

Figure S12. *^{1}H and ^{13}C NMR spectra of 4, 4'- Dimethylbiphenyl*

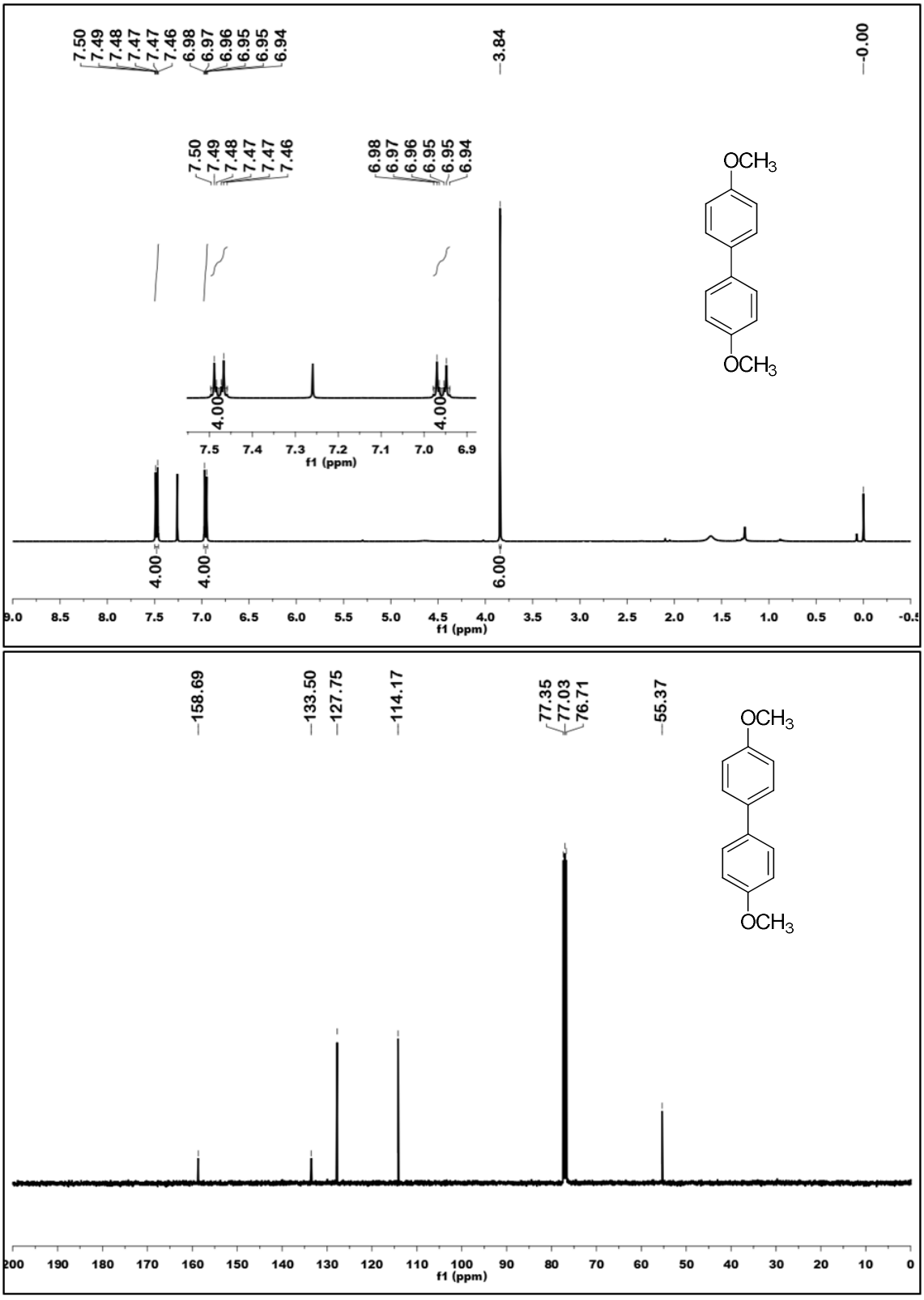

Figure S13. *^{1}H and ^{13}C NMR spectra of 4, 4'- Dimethoxybiphenyl*

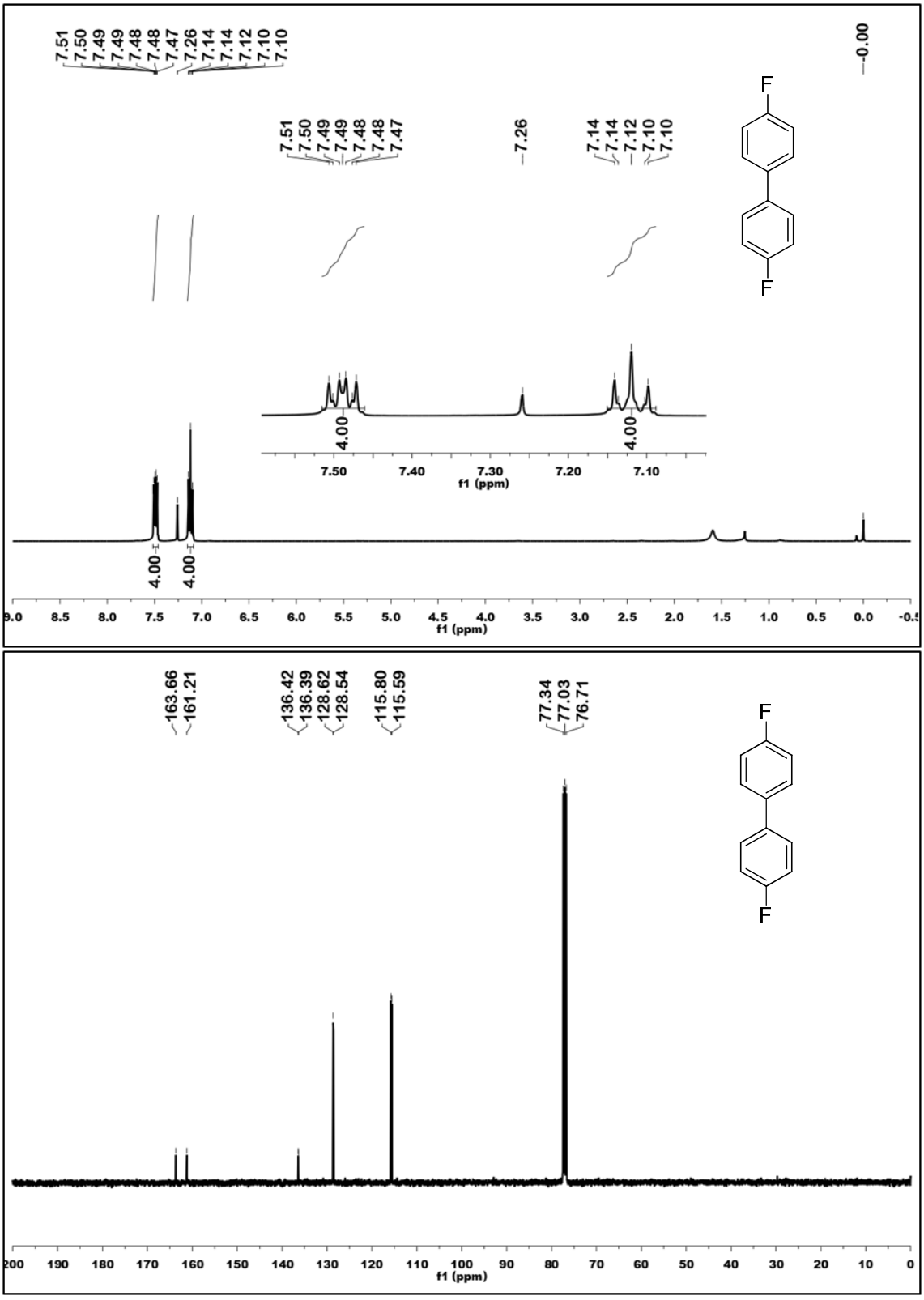

Figure S14. *^{1}H and ^{13}C NMR spectra of 4, 4'- Difluorobiphenyl*

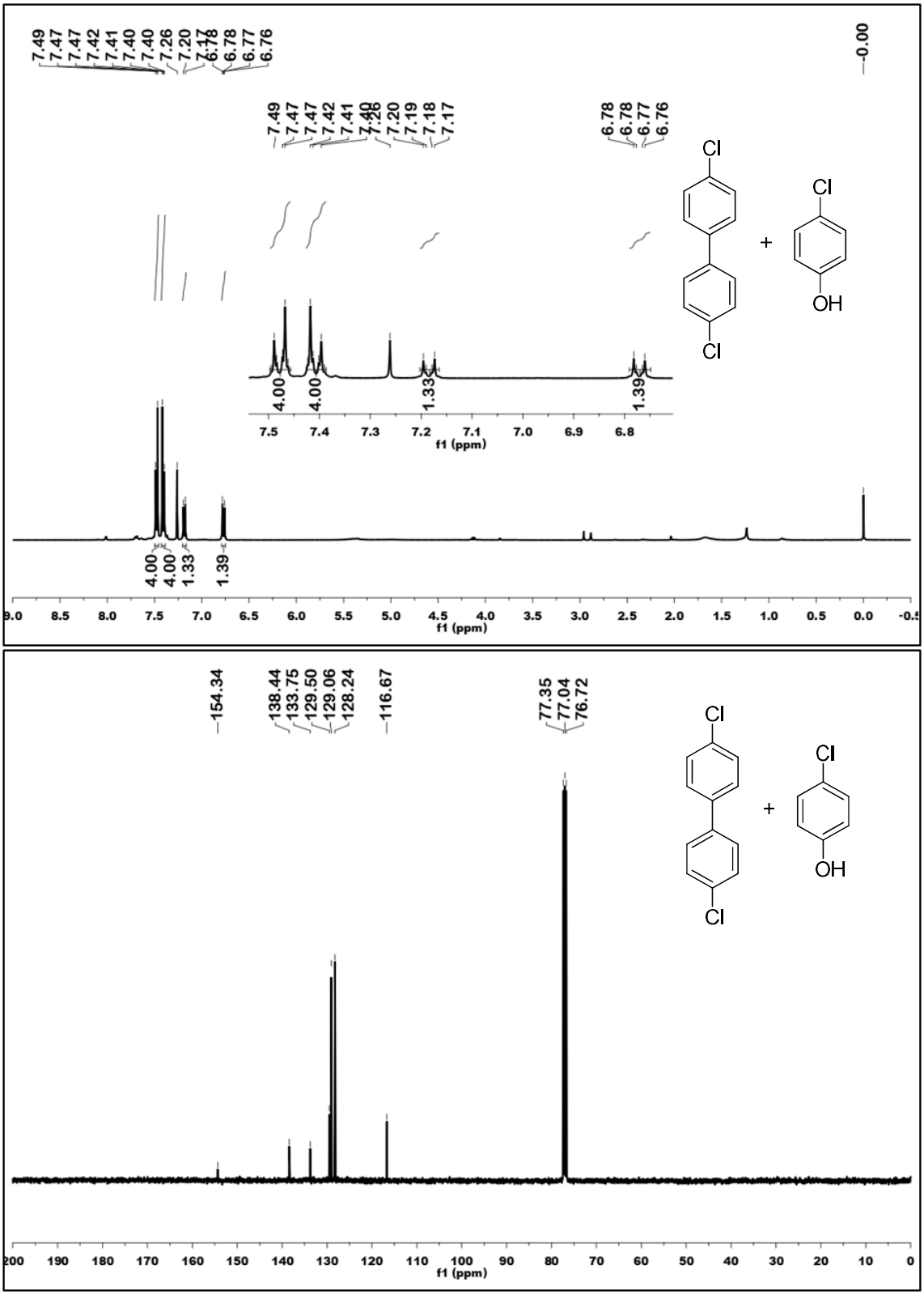

Figure S15. *^{1}H and ^{13}C NMR spectra of 4,4'-Dicholorobiphenyl with 4-chloro phenol*

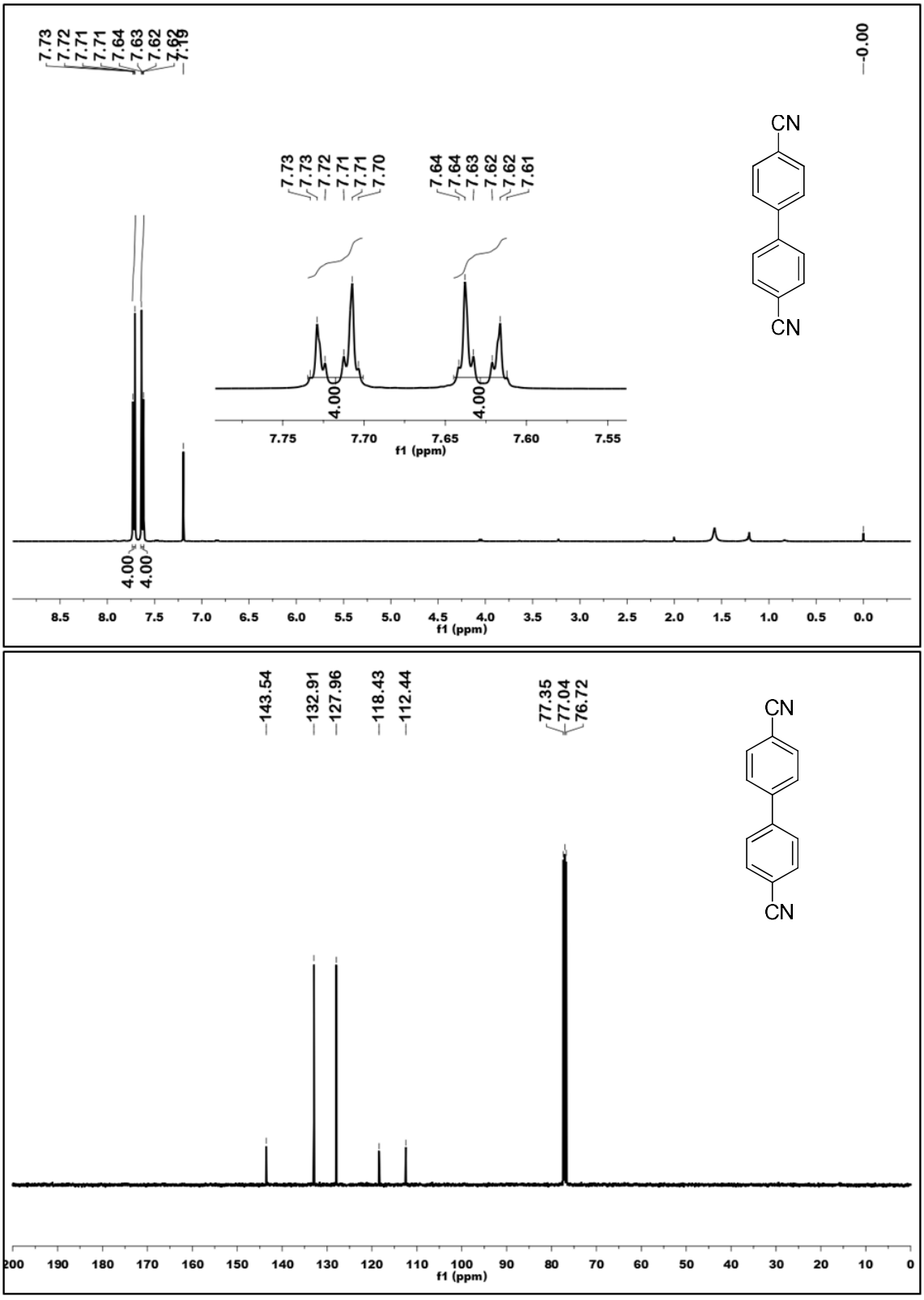

Figure S16. *^{1}H and ^{13}C NMR spectra of 4, 4'- Dicyanobiphenyl*

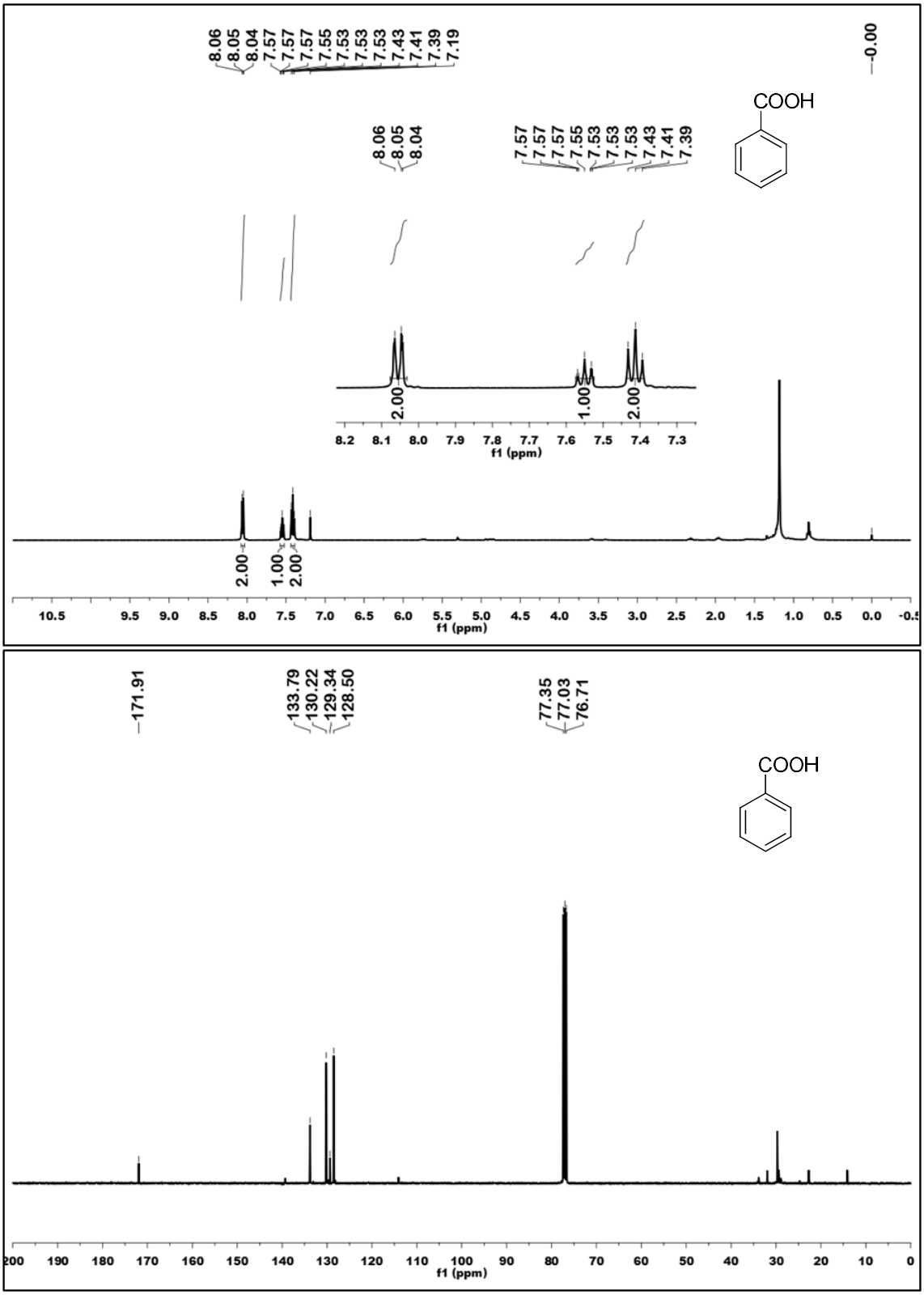

Figure S17. *^{1}H and ^{13}C NMR spectra of Benzoic acid*

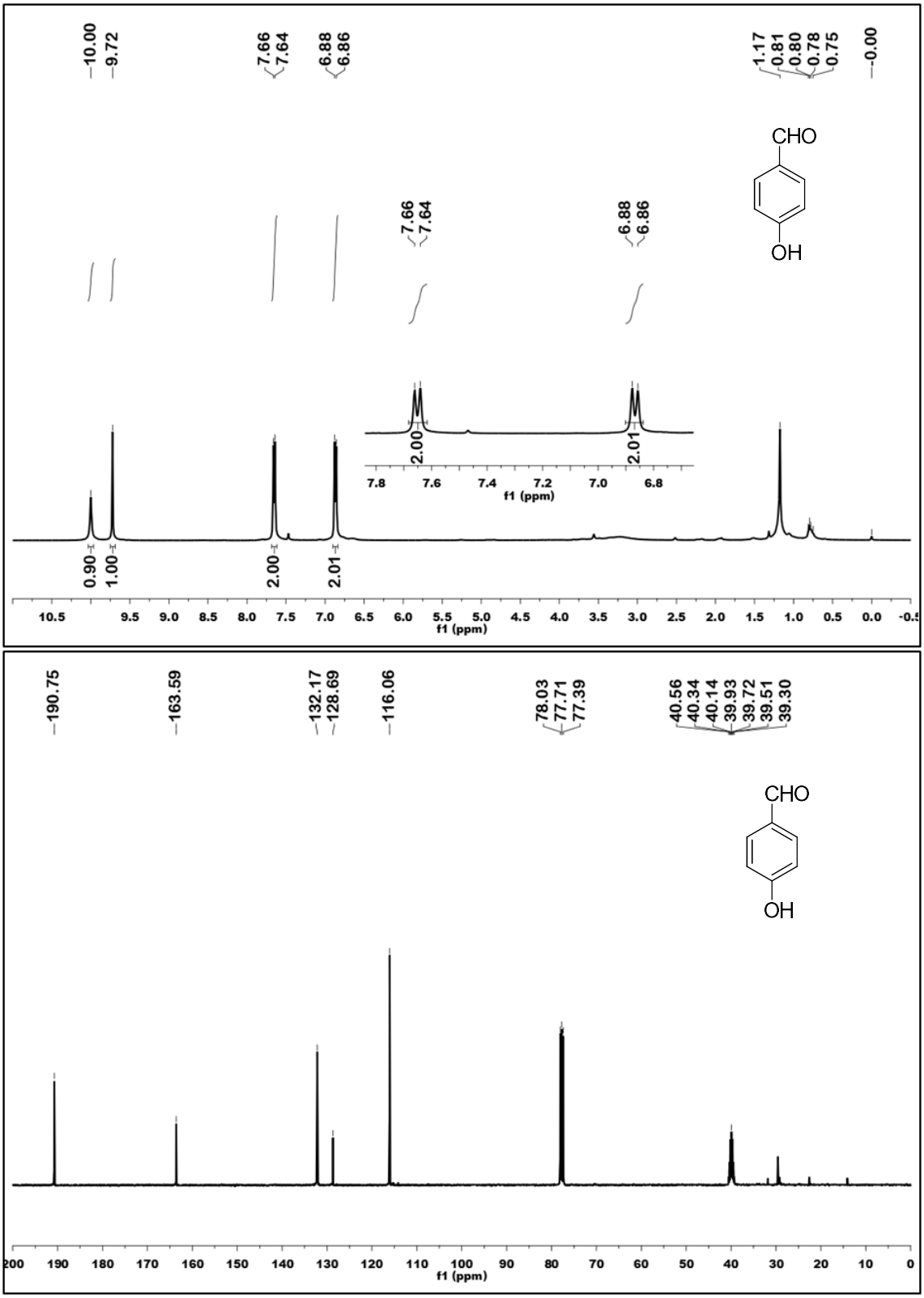

Figure S18. *^{1}H and ^{13}C NMR spectra of 4 - Hydroxybenzaldehyde*

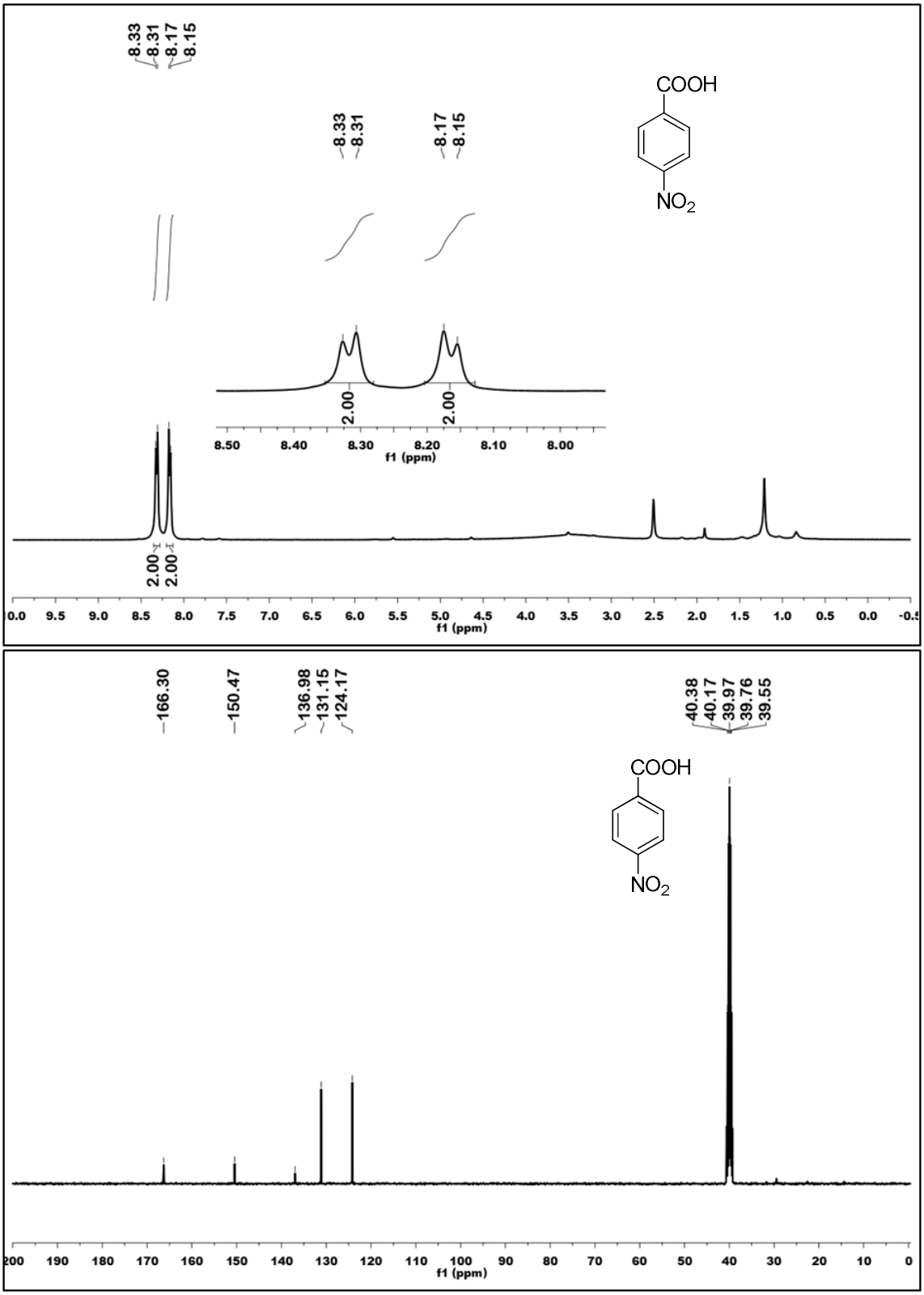

Figure S19. *^{1}H and ^{13}C NMR spectra of 4 –Nitrobenzoicacid*

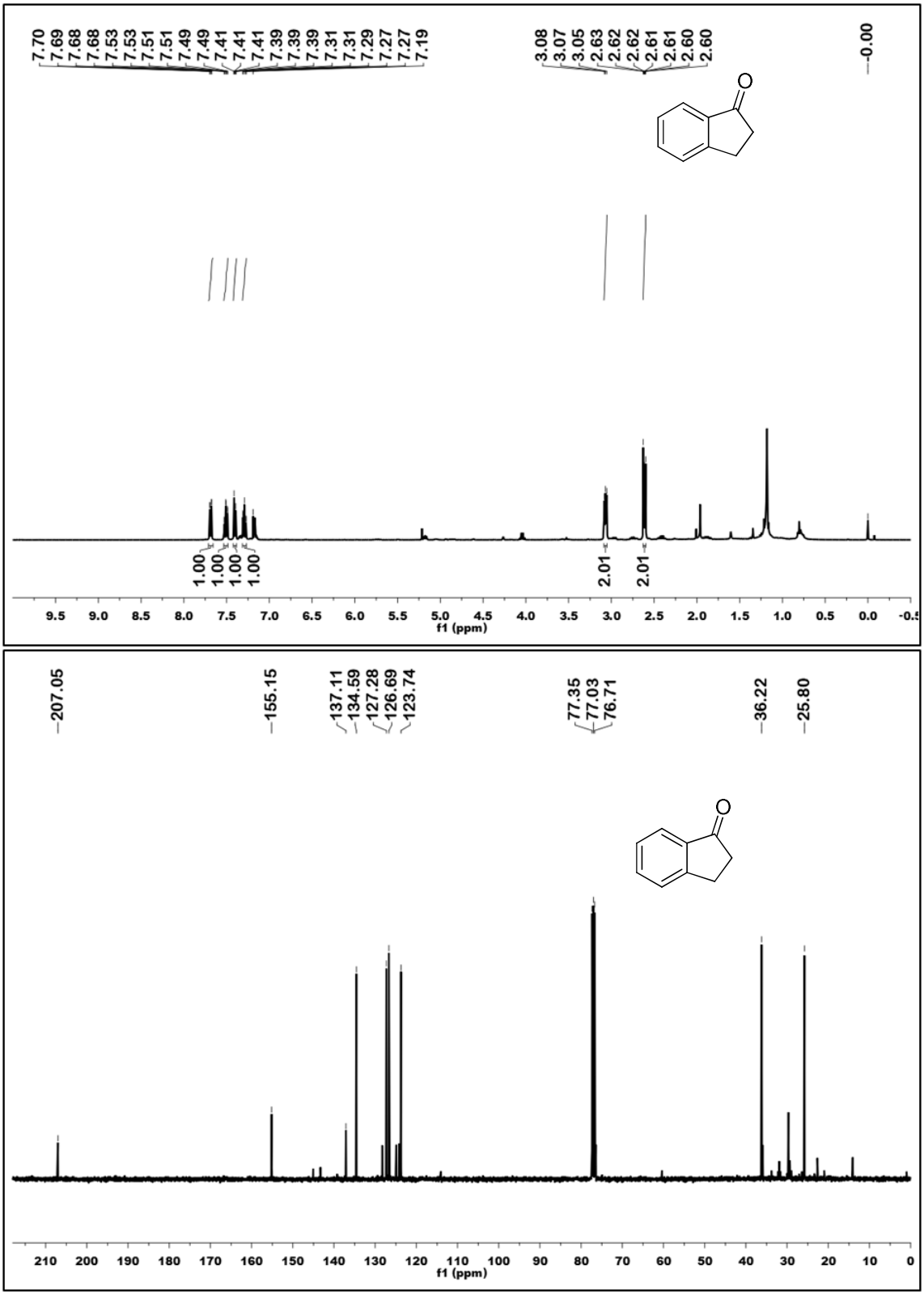

Figure S20. *^{1}H and ^{13}C NMR spectra of 1-indanone*

References:

1. A. Murugadoss, and H. Sakurai, *J. Mol. Catal. A Chem.*, 2011, 341, **1-2**, 1-6.
2. S. I. Zabinsky, J. J. Rehr, A. Ankudinov, R. C. Albers, and M. J. Eller, *Phys. Rev. B.*, 1995, **52**, 2995–3009.
3. B. Ravel, and M. Newville, *J. Synchrotron Radiat*., 2005, **12**, 537–541.
4. K. Paul Reddy, K. Jaiswal, B. Satpati, C. Selvaraju and A. Murugadoss, *New J. Chem.,* 2017, **41**, 11250-11257.
5. M. A. Mahmoud, B. Garlyyev, and M. A. El-Sayed, *J. Phys. Chem.* C, 2013, **117**, 21886-21893.